

Microenvironmental Investigation of Polymer-Bound Fluorescent Chelator by Fluorescence Microscopy and Optical Spectroscopy

Ying Wang,[†] Simion Astilean,^{‡,§} Gilad Haran,[†] and Abraham Warshawsky^{*,†}

Departments of Organic Chemistry and Chemical Physics, The Weizmann Institute of Science, Rehovot, 76100, Israel

8-Hydroxyquinoline-5-sulfonic acid (HQS) was immobilized onto a strong-base anion-exchange resin AG MP-1 for the purpose of microenvironment investigation, resin characterization, and possibly sensing cadmium. The maximum loading of HQS was found to be 0.9340 mmol/g of AG MP-1. A plateau for Cd complex capacity was already obtained for 0.5500 mmol of HQS/g of AG MP-1. A minicolumn experiment showed an influence of influent Cd concentration on column capacity. IR and Raman spectra proved an electrostatic mode for HQS immobilization and Cd complex formation. UV spectroscopy showed significant differences between solution and solid state for both HQS and Cd complex. A fluorescence microscopy technique was used for fluorescence spectral measurement, microdistribution imaging, and study of photobleaching of HQS and the HQS–Cd complex in the resin phase. The fluorescence of immobilized HQS was found to be red-shifted with regard to the solid-state HQS. The microdistribution of uncomplexed and Cd-complexed AG MP-1-HQS was directly visualized by fluorescence imaging, showing a nonuniform distribution. Cadmium complexation modifies the fluorescence emission of uncomplexed AG MP-1-HQS, exhibiting an increased and red-shifted emission. Significant photobleaching of the fluorescence from the Cd complex was recorded, indicating the occurrence of photochemical reactions within the microenvironment of the resin phase.

The idea of a chromophoric “chelate-forming” resin, which is capable of selective removal and recovery of environmentally and economically important metal ions from aqueous solutions, is relatively new.^{1–8} Most of the studies evaluating the use of chromophoric “chelate-forming” resins focus on the efficiency in

separation and preconcentration of metal ions from aqueous solutions. Few studies are devoted to the microenvironment, microdistribution, and microscopic optical properties of the resin using optical microscopy. In the present study, our first aim is to probe the microdistribution of extractant and metal complex using fluorescence microscopy measurement, with the hope of pushing the limits of metal analysis to the microscale. Our second aim is to explore the interaction among chelator, metal complex, and polymeric support by the use of IR, Raman, and UV spectroscopy.

Fluorescence and photobleaching studies under a microscope are very attractive methods for exploring molecular association structures and processes on the microscale. Indeed, since a laser beam can be focused onto a small diffraction-limited spot, such measurements can provide information about micrometer-size zones in polymeric films and microcrystals.^{9,10} Spatial resolution and signal quality can be even further improved to some extent by introducing two-photon excitation.¹¹ Two-photon fluorescence microscopy is applied here for the first time for the characterization of a chromophoric “chelate-forming” resin.

Considering one of the most frequently used chelating agents, 8-hydroxyquinoline (HQ), and its fluorescence properties (upon complexing with metal ions), an analogue of HQ containing an acid function, 8-hydroxyquinoline-5-sulfonic acid (HQS) was chosen to be immobilized onto the strong-base anion-exchange resin AG MP-1. Owing to the presence of the sulfonic acid group, HQS is easily immobilized from aqueous solution onto the positively charged strong-base anion-exchange resin by electrostatic interaction. This is a very facile method since the amounts of immobilized HQS can be easily varied, sparing time-consuming procedures needed for covalently linking HQS to the skeleton of the resin.

HQS in metal-free solution shows virtually no native fluorescence but forms fluorescent complexes with a large number of metal ions. Detailed fluorescence spectroscopy of 42 different metal–HQS complexes, as well as the use of these complexes for detection in ion chromatography^{12,13} and capillary zone electrophoresis,^{14–16} has been reviewed. The chelation and pre-

* Corresponding author: (e-mail) cowaresha@wicc.weizmann.ac.il; (tel) 972-8-9342242/3; (fax) 972-8-9344142.

[†] Department of Organic Chemistry.

[‡] Department of Chemical Physics.

[§] On leave from the Optics and Spectroscopy Department, Babes-Bolyai University, 3400 Cluj-Napoca, Romania.

- (1) Tewari, P. K.; Singh, A. K. *Analyst* **1999**, *124*, 1847–1851.
- (2) Sérgio, L.; Ferreira, S. L. C.; de Brito, C. F. *Anal. Sci.* **1999**, *15*, 189–191.
- (3) Sutton, R. M. C.; Hill, S. J.; Jones, P. J. *J. Chromatogr., A* **1996**, *739*, 81–86.
- (4) Olbrych-Sleszynska, E.; Brajter, K.; Matuszewski, W.; Trojanowicz, M.; Frenzel, W. *Talanta* **1992**, *39* (7), 779–787.
- (5) Pesavento, M.; Biesuz, R. *React. Polym.* **1991**, *14*, 239–250.
- (6) Pesavento, M.; Profumo, A.; Riolo, C.; Soldi, T. *Analyst* **1989**, *114*, 623–626.
- (7) Pesavento, M.; Profumo, A.; Biesuz, R. *Talanta* **1988**, *35* (6), 431–437.

- (8) Nakayama, M.; Chikuma, M.; Tanaka, H.; Tanaka, T. *Talanta* **1982**, *29*, 503–506.
- (9) Yoshikawa, H.; Masuhara, H. *J. Photochem. Photobiol. C: Photochem. Rev.* **2000**, *1*, 57–78.
- (10) Hou, Y.; Bardo, A. M.; Martinez, C.; Higgins, D. A. *J. Phys. Chem. B* **2000**, *104*, 212–219.
- (11) Springer, G. H.; Higgins, D. A. *Chem. Mater.* **2000**, *12*, 1372–1377.
- (12) Soroka, K.; Vithanange, R. S.; Phillips, D. A.; Walker, B.; Dasgupta, P. K. *Anal. Chem.* **1987**, *59*, 629–636.

concentration of heavy metals from seawater by solid-phase extraction technology in the use of HQS has been evaluated.^{17,18} Also, optical fiber sensors for As(III), Mg(II), Zn(II), and Cd(II) were prepared.¹⁹ The spectra of HQS and transition-metal complex doped sol-gel matrix were also reported.²⁰ The fluorescence spectrum and response provided the average properties of these sensing matrixes. However, the microdistribution of HQS and its Cd complex, and the fluorescence emission from microscale zones in which HQS and its Cd complex deposit in the resin phase, are unexplored as yet. Fluorescence microspectroscopic measurements may allow us to concurrently correlate resin morphology and topography with the fluorescence image, local fluorescence spectra, and fluorescence photobleaching. In particular, studies of photobleaching reactions of the fluorescent chelator and its Cd complex will aid in understanding the chemistry occurring within the sensors and allow development of improved sensors.

In this paper, the loading of HQS onto AG MP-1 anion-exchange resin was studied. Cd complexation was carried out by both batch and minicolumn experiments. IR and Raman spectra were very efficient in following the immobilization of HQS and Cd complexation. UV spectra differ and depend on whether HQS is in the solution, in the solid state, or immobilized on AG MP-1. Fluorescence of HQS in the solid state and in the resin-immobilized HQS also shows significant differences, which are attributed to the different associated forms (hydrogen-bonded HQS in the solid state, electrostatic-bonded HQS in the polymer phase). Cd complexation modifies both UV spectrum and fluorescence of the immobilized HQS. Fluorescence imaging illustrates that HQS and its Cd complexes are unevenly distributed in the resin phase. Fluorescence intensity time traces show that some chemical reactions occurred within the resin microenvironment.

EXPERIMENTAL SECTION

Materials and Reagents. Analytical grade AG MP-1 (75–150 μm) was obtained from Bio-Rad. All solutions were prepared using distilled deionized water (Milli-Q system, Millipore). Analytical grade reagents were used throughout. A solution of 8-hydroxyquinoline-5-sulfonic acid (Aldrich Chemical Co.) at 1.723×10^{-3} mol/L was freshly prepared. A stock solution of cadmium was obtained by dissolving cadmium perchlorate hydrate (Aldrich Chemical Co.) in water, and the concentration was detected by AAS measurements. All solutions including pH 6.23 phosphate buffer were stored in plastic bottles.

Apparatus. Samples were characterized by scanning electron microscopy (SEM). SEM images were obtained on a JEOL JSM 6400 microscope. Infrared spectra from 400 to 4000 cm^{-1} were obtained on a Nicolet 460 single-beam infrared Fourier transform spectrophotometer (FT-IR) using KBr pelleted samples. Raman spectra were recorded on a Renishaw micro Raman imaging

microscope with 633-nm laser excitation. The electronic absorption spectra were scanned on a Jasco V-570 UV/vis/NIR spectrophotometer. Solution fluorescence was detected on a SLM 8100 spectrofluorometer. Cadmium in the solutions was analyzed with a Perkin-Elmer 5100 atomic absorption spectrophotometer (AAS).

Fluorescence Microscopy Measurements. The home-built fluorescence microscopy system used here was based on a mode-locked Ti-sapphire laser, providing femtosecond duration pulses at a repetition rate of 76 MHz and wavelength centered at 800 nm, which served as a two-photon excitation source. The beam from this laser was sent into a microscope through the objective, and the two-photon excited fluorescence was collected by the same objective lens and filtered by a combination of a dichroic mirror and a color filter. The average excitation power at the diffraction-limited spot was 1 mW. For excitation and collection of fluorescence we used either an oil immersion objective (100 \times , NA = 1.3) or a dry objective (10 \times , NA = 0.25). Detection was carried out either by a photon-counting avalanche photodiode or by a CCD camera coupled to a spectrograph. For fluorescence imaging, the sample was mounted on a scanning stage. After the fluorescence image was obtained, photobleaching measurements or fluorescence spectra of a small volume at a particular position in the image were carried out.

At a high excitation power of 4.11 mW and long acquisition time of 10 s, the autofluorescence of the AG MP-1 resin itself can be detected, with a maximum emission at 487 nm. However, upon reducing laser power to 1 mW and 1-s acquisition time, autofluorescence is not detected. Thus, no background fluorescence was obtained from AG MP-1 in all subsequent experiments.

Immobilization of HQS on AG MP-1. Approximately 1 g of AG MP-1 resin was thoroughly mixed with 25 mL of 0.36 mol/L NaOH solutions containing various amounts of HQS, respectively. The strong basic conditions are required to increase the solubility of HQS in aqueous solution and for interaction with the AG MP-1 resin. The mixtures were allowed to shake for 24 h at 180 rpm until equilibrium was reached. The resin was filtered. The supernatant was analyzed by the addition of Cd to form fluorescent complex. The filtered resin was then shaken with 30 mL of water at 180 rpm for 5 h. To ensure the lowest leakage of the immobilized HQS from AG MP-1, the water-washing procedure was repeated seven times. Although HQS was each time found in the aqueous phases, the leakage was very small and could be ignored. Therefore, the amount of immobilized HQS was calculated only from the difference between the initial amount of HQS and the residual HQS in the supernatant after immobilization.

Cd Binding: Batch Equilibration Experiments (Table 1). AG MP-1-immobilized HQS was filtered from water, washed with absolute methanol, and dried under vacuum at room temperature for 10 h to prevent oxidation of the immobilized HQS. The immobilized HQS-AG MP-1 was stored in dark glass bottles under argon.

Under continuous mixing on a shaker at 180 rpm, 30.00 mL aliquots of test solutions containing 105.8 ppm Cd were equilibrated for 24 h with various amounts of AG MP-1-HQS (accurately weighed; see Table 1). After filtration of these resins, Cd in the filtrate was determined by AAS. The amounts of Cd per gram of AG MP-1-HQS were calculated according to the equation²¹

$$Q = (C_0 - C)V/mW$$

(13) Dasgupta, P. K.; Soroka, K.; Vithanage, R. S. *J. Liq. Chromatogr.* **1987**, *10* (15), 3287–3319.

(14) Ye, L. W.; Wong, J. E.; Lucy, C. A. *Anal. Chem.* **1997**, *69*, 1837–1843.

(15) Swaile, D. F.; Sepaniak, M. J. *Anal. Chem.* **1991**, *63*, 179–184.

(16) Zhu, R. H.; Kok, W. T. *Anal. Chim. Acta* **1998**, *371*, 269–277.

(17) Abollino, O.; Mentasti, E.; Porta, V.; Sarzanini, C. *Anal. Chem.* **1990**, *62*, 21–26.

(18) Abollino, O.; Aceto, M.; Sarzanini, C.; Mentasti, E. *Anal. Chim. Acta* **2000**, *411*, 223–237.

(19) Zhang, Z. J.; Seitz, W. R. *Anal. Chim. Acta* **1985**, *171*, 251–258.

(20) Arbuthnot, D.; Wang, X. J.; Knobbe, E. T. *J. Non-Cryst. Solids* **1994**, *178*, 52–57.

Table 1. Cadmium Complexing Capacities on AG MP-1-HQS

mmol of HQS in solution	mmol of HQS/g of AG MP-1	wt of AG MP-1-HQS (mg) ^a	Cd on AG MP-1-HQS (Q , mmol/g)	mmol of Cd bound/mmole of HQS
0	0	396.5 ^b	0.067 ^c	
0.0630	0.05548, 0.188 ^d	201.63	0.1067	1.920
0.1753	0.1625, 0.600 ^d	225.98	0.1046	0.644
0.6215	0.5500	217.00	0.1227	0.223
1.2332	0.8895	216.40	0.1231	0.138
1.3206	0.9548	215.05	0.1239	0.130
2.3250	0.9340	207.45	0.1285	0.138
2.6656	0.9347	220.45	0.1209	0.129

^a Weight of AG MP-1 HQS for Cd(II) complexing experiments. ^b Weight of AG MP-1 only. ^c Cd adsorbed directly on the AG MP-1 resin. ^d HQS loaded from neutral water.

where Q is the amount of Cd per gram of AG MP-1 (mmol/g); C_0 and C are the concentrations of Cd in the initial solution and in the aqueous solution after complexation with the immobilized HQS for 24 h, respectively (in mg/mL); V is the volume of the aqueous solution (ml) and m is the amount of AG MP-1-HQS(g); and W is the molecular weight of HQS.

Minicolumn Experiments. About 0.5 g of swollen AG MP-1-HQS (0.5500 mmol/g of AG MP-1) was slurry-packed into a minicolumn (1.0 mL of a sterile single-use Plastipak syringe) fitted with 25- μ m polyethylene frits as bed supports. Solutions were delivered by a Masterflex L/S digital drive (Cole-Parmer model 7523-40) and an easy-load pump head II. The minicolumn was first washed with water and then conditioned with 0.05 mol/L ammonium acetate for 5 min. The uptake of Cd was studied at pH 7.0 with influent flow rate of 1.0 mL/min. The reason for using pH 7.0 as a reference pH²² is to simulate natural water and to complex Cd by AG MP-1-HQS. The effluent from the column was collected continuously every 30 min for 10 ppm Cd and 20 min for 30 ppm Cd influents and then analyzed by AAS measurements.

RESULTS AND DISCUSSION

Loading of HQS on AG MP-1. As shown in Table 1, the loading of HQS on AG MP-1 increases linearly with increasing HQS concentrations in the aqueous phases before reaching a plateau value. The saturation value of the loaded HQS (0.9340 mmol/g of AG MP-1) is considerably lower in comparison to the saturation value for chloride ions (4.2 mequiv/g of AG MP-1). The lower affinities of AG MP-1 to HQS anions are due to steric hindrance exerted by the HQS molecules; subsequently, they decrease the accessibility of the sulfonic acid group of HQS to the quaternary ammonium group on AG MP-1. Another reason is the competition of hydroxyl and HQS anions. To illustrate this point, an experiment was performed by immobilization of HQS from neutral water. The results are also shown in Table 1. The immobilization from water is more effective than that from basic condition. This shows that ion exchange between Cl^- and OH^- further prevents the access of more HQS anions to the quaternary ammonium groups on AG MP-1.

Cd Complexing Capacity. Batch Experiments. Table 1 also lists Cd complexing capacities (Q) on AG MP-1 and AG MP-1-HQS. The amount of Cd adsorption on AG MP-1 is smaller than

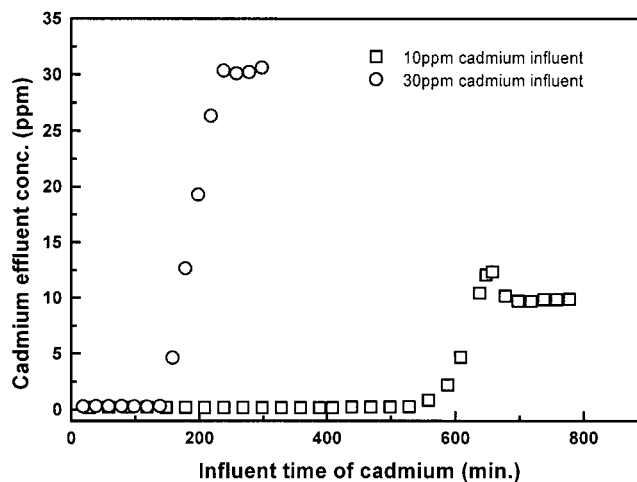


Figure 1. Breakthrough curves on AG MP-1-HQS for 10 and 30 ppm Cd solutions.

that of the AG MP-1-HQS complex. Therefore, it is necessary to immobilize HQS unto AG MP-1 for the removal of Cd from water. No striking differences are apparent from the lowest to the highest loading concentration of HQS. An almost identical Cd capacity is obtained in the range from 0.1625 to 0.9347 mmol/g of AG MP-1. The ratio between Cd bound and HQS was calculated and is shown in Table 1. The ratio in relation to the available HQS group dropped from 1.92 for 0.05548 mmol of HQS/g of AG MP-1 to 0.129 for 0.9347 mmol of HQS/g of AG MP-1. That is, we observed excess binding efficiency for the lowest loading of HQS and lower binding efficiency for the higher loading of HQS. This can be explained in the first case by Cd binding via two mechanisms, by HQS complexation and by precipitation with OH^- as $\text{Cd}(\text{OH})_2$. In the highest loading of HQS, the lower efficiency is due to low accessibility of Cd caused by many of the immobilized HQS molecules being sterically hindered either by polystyrene itself or by other HQS molecules. In view of the above, we chose 0.5500 mmol of HQS/g of AG MP-1 for all further studies.

Column Capacity. The uptake of Cd by AG MP-1-HQS was studied in order to determine whether Cd concentration would affect column capacity. Figure 1 shows breakthrough curves on AG MP-1-HQS for 10 and 30 ppm Cd solutions, respectively. Both of the breakthrough curves have an early-time baseline region, pointing to quantitative binding of the influent Cd. Comparing Cd effluent versus influent concentrations, the column reached equilibrium after 12 h for 10 ppm Cd and 4 h for 30 ppm Cd. The

(21) Salih, B.; Denizli, A.; Engin, B.; Piskin, E. *React. Funct. Polym.* **1995**, *27*, 199–208.

(22) Howard, M.; Jurbergs, H. A.; Holcombe, J. A. *J. Anal. At. Spectrom.* **1999**, *14*, 1209–1214.

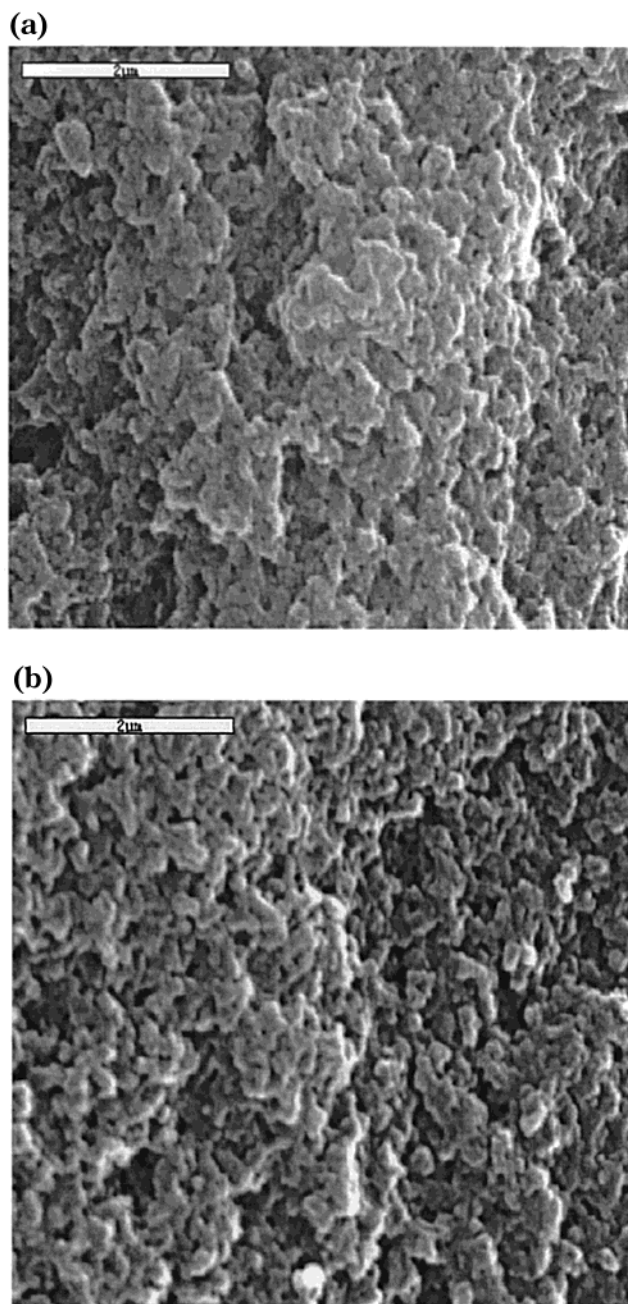


Figure 2. SEM images from (a) AG MP-1 and (b) immobilized HQS on AG MP-1.

total amount of Cd on AG MP-1 was determined by the difference between the influent amount of Cd and the integration of the breakthrough curves as shown in Figure 1. The Cd retention on the columns is 0.0535 mmol of Cd/g of AG MP-1-HQS for the 10.0 ppm influent and 0.063 85 mmol of Cd/g of AG MP-1-HQS for the 30.0 ppm influent.

Scanning Electron Microscopy. The surface morphology of the AG MP-1 resin and AG MP-1-HQS was examined by SEM and is shown in panels a and b of Figure 2, respectively. Both resins show highly porous structures. As may be expected, immobilization of HQS does not induce any change of the structure. Consequently, the AG MP-1-HQS resin retains high accessibility of the functional groups, ideal for efficient metal binding.

Infrared Spectroscopy. IR spectra can provide information on the mode of attachment of HQS and its metal complexes on

the AG MP-1 resin. Table 2 lists the main IR absorption frequency assignments for HQS (s), AG MP-1-HQS, and Cd-complexed AG MP-1-HQS, respectively. The two strong bands of HQS (s) which appear at 1604 and 1556 cm^{-1} can be attributed to the quinoline $\nu_{\text{C}=\text{N}}$. The changes of the location of the two bands to 1650 and 1548 cm^{-1} indicate the attachment of HQS onto AG MP-1 resin. The bands of HQS (s) appearing at 1310 and 1186 cm^{-1} can be ascribed to asymmetric and symmetric vibrations, respectively, of $\nu_{\text{O}=\text{S}=\text{O}}$.²³ Changes in these bands provide evidence for the ionic interaction between sulfonate groups of HQS and the ammonium groups on the resin. In addition, HQS (s) has a very strong absorption band at 861 cm^{-1} assigned to S–O stretching mode. Sakurai and co-workers²³ found this band at 907 cm^{-1} . The other IR bands of HQS, appearing at 771 and 500 cm^{-1} , have been related to ring vibration of HQS and C–O in-plane bending.^{24,25} Evidently, both changes in the S–O stretching and ring vibration of HQS support and prove the contention that HQS is immobilized on AG MP-1 by an electrostatic mode.

The immobilized HQS contains two coordination sites, namely, the hydroxyl anion and the tertiary nitrogen of the quinoline ring. The coordination sites involved in binding Cd can be determined by comparison of the various infrared spectra as shown in Table 2. The changes of two bands at 1650 and 1548 cm^{-1} show that the coordination of Cd takes place through the nitrogen atom of the immobilized quinoline molecule. A new peak appearing at 1087 cm^{-1} in the Cd complex is attributed to C–O vibration as suggested in the literature²⁶ by Charles and co-workers, and its appearance is consistent with the absorption band for many metal-8-hydroxyquinoline chelates.²⁶ This is strongly supportive of the contention that the 1087- cm^{-1} band results from diatomic vibration of C–O group, indicated in Scheme 1 as bond A. In summary, all changes in band locations in the IR spectra of Cd-complexed AG MP-1-HQS are consistent with Cd complex formation.

Raman Characterization. Prior to performing fluorescence measurements, the formation of the Cd complex on the AG MP-1-HQS resin was also confirmed by Raman spectroscopy. No Raman spectroscopy data of the Cd–HQS complex have been published before. For the purpose of a reference, we prepared the solid-state HQ–Cd complex as per the literature.²⁵ Table 3 lists some main Raman frequencies. It can be seen that Raman spectra are very sensitive to the existence of Cd complexes. That is, complexation brings about considerable changes in the Raman frequencies and intensities regardless of whether Cd is in the form of HQ–Cd or immobilized HQS–Cd. First, let us examine the shifts in two similar Raman bands at 1382 cm^{-1} for HQ and at 1347 cm^{-1} for immobilized HQS. Obviously, complexation shifts the two bands to 1368 and 1352 cm^{-1} , respectively, and increases their intensities. Second, after Cd complexation, the two bands appearing at 720 and 731 cm^{-1} on AG MP-1-HQS converge to a single band at 738 cm^{-1} . A similar shift (from 715 to 732 cm^{-1}) was also observed for the HQ–Cd complex. Similarly, the band at 475 cm^{-1} shifts to 501 cm^{-1} in HQ–Cd and the band at 499 cm^{-1} shifts to 508 cm^{-1} in the immobilized HQS–Cd. All those

(23) Sakurai, K.; Douglas, E.; Macknight, W. J. *Macromolecules* **1993**, *26*, 208–212.

(24) Magee, R. J.; Gordon, L. *Talanta* **1963**, *10*, 851–859.

(25) Ohkaku, N.; Nakamoto, K. *Inorg. Chem.* **1971**, *10* (4), 798–805.

(26) Charles, R. G.; Freiser, H.; Friedel, R.; Hilliard, L. E.; Johnston, W. D. *Spectrochim. Acta* **1956**, *8*, 1–8.

Table 2. Some Fundamental IR Frequencies (cm⁻¹) on Solid Samples^a

HQS (s)	AG MP-1 –HQS	Cd complexed AG MP-1-HQS	assignments
1604 (s), 1556 (s)	1650 (br, s)	1650 (br, m)	C=N stretching
	1548 (m)	1561 (m)	
1310 (s)	1326 (m)	1326 (m)	O=S=O asymmetric stretching ²³
1186 (s, br)	1182 (m)	1178 (m, br)	O=S=O symmetric stretching ²³
		1087 (m)	C–O bond of HQS ²⁶
861 (s)	856 (w)	850 (w)	S–O stretching ²³
771 (m)	792 (w)	781 (w)	ring vibration from HQS ²⁴
500 (m)	500 (w)	504 (w)	C–O in-plane bending ²⁵

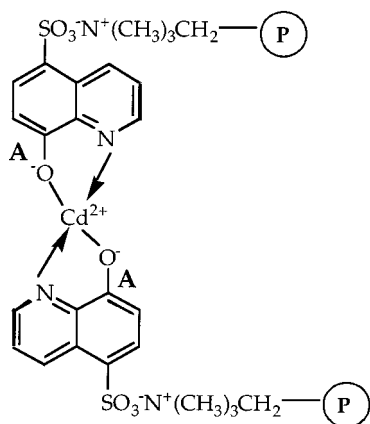
^a s, strong; m, medium; w, week.

Table 3. Some Fundamental Raman Frequencies (cm⁻¹) on Solid Samples^a

HQ	HQ-Cd complex	AG MP-1-HQS	Cd-complexed AG MP-1-HQS	assignments
1382 (m)	1368 (s)	1347 (m)	1352 (s)	quinoline ring stretching
715 (s)	732 (w)	720 (m)	738 (m)	quinoline ring vibration
		731 (m)		
475 (m)	501 (s)	499 (m)	508 (m)	C–O in plane bending

^a s, strong; m, medium; w, week.

Scheme 1



shifts provide further evidence for the formation of the Cd complex.

UV Spectroscopy. Figure 3 shows electronic absorption spectra of AG MP-1, HQS in buffer (pH 6.64 K₂HPO₄–KH₂PO₄), in 0.15 mol/L NaOH, in the solid state, and on AG MP-1, respectively. AG MP-1 itself has a maximum absorbance around 325 nm. HQS shows spectral variations in varying matrixes. In a pH 6.64 buffer, two absorption bands appear. One is located at 254 nm; the other appears at 310 nm. In 0.15 mol/L NaOH, the maximum absorption appears at 360 nm. In the solid state, HQS exhibits a broad band appearing in the range of 347–380 nm. After immobilization on AG MP-1, HQS shows significant changes in its spectrum, with one maximum located at 343 nm, while another maximum is red-shifted to the 375–400-nm region.

In aqueous solution, the absorbance spectra of HQS are influenced by the pK_a values of the N⁺H and OH groups (3.93 and 8.42, respectively).²⁷ At a pH value of ~7, the neutral form is predominant (A, Chart 1), with two bands appearing at 254 and

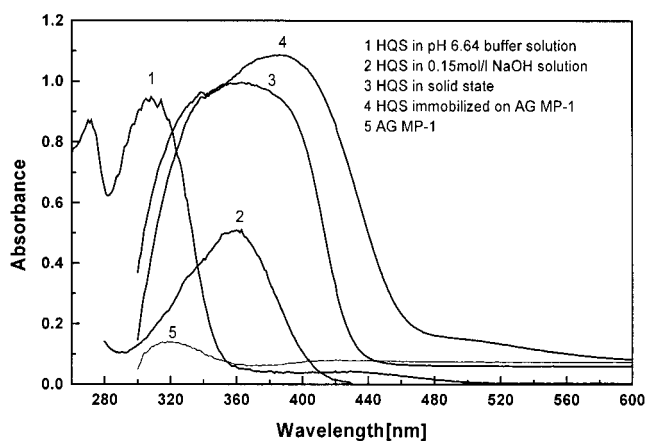
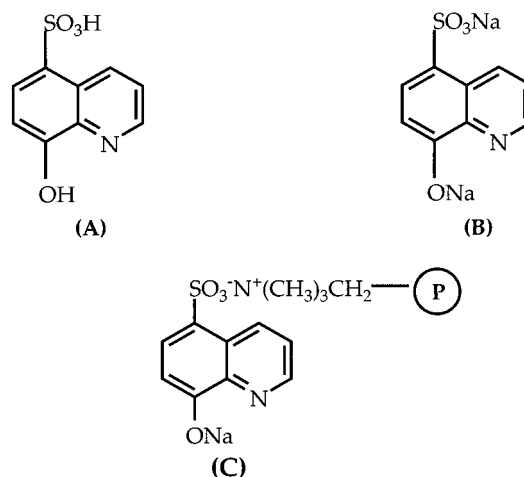


Figure 3. Electronic absorption spectra of AG MP-1, HQS in buffer (pH 6.64 K₂HPO₄–KH₂PO₄), in 0.15 mol/L NaOH, in the solid state, and on AG MP-1.

Chart 1



310 nm. In 0.15 mol/L NaOH, HQS exists almost exclusively in the anionic form (B, Chart 1) with an absorption maximum at

(27) Smith, R. M.; Martell, A. E. *Critical Stability Constants*; Plenum Press: New York, 1975; Vol. 2, p 227.

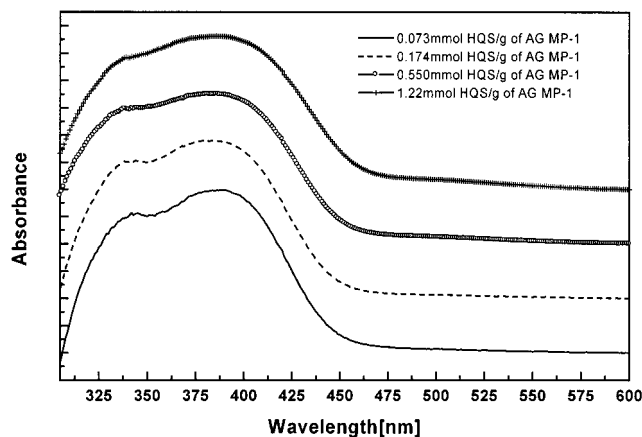


Figure 4. Normalized and offset (normalization at 350 nm and offset 0.4 at 600 nm) electronic absorption spectra of the immobilized HQS with varying amounts of HQS on AG MP-1.

360 nm. Structural studies of sodium 8-hydroxyquinoline-5-sulfonate dihydrate²⁸ suggest that HQS hydrate is mostly hydrogen-bonded in the solid state and the proton in this bond originates from the SO_3H group and not from the phenolic OH group. Consequently, the broad absorption band in the region of 347–380 nm is due to the associated form of HQS. Since HQS was immobilized from 0.36 mol/L NaOH, the predominant form is deprotonated quinolate (C, Chart 1). Spectral analysis of HQS in NaOH solution shows that the conjugation of the hydroxyl anion with the quinoline ring causes the two bands at 254 and 310 nm (in the neutral form) to shift to a single band at 360 nm (quinolate). Therefore, it is reasonable to state that the band in the region of 375–400 nm is attributed to the deprotonated quinolate (C, Chart 1). The increase in conjugation via the fixed negatively charged phenolic oxygen with the quinoline ring, and the interaction between AG MP-1 and immobilized HQS, are responsible for the appearance of bands at 370–400 and 343 nm. Samples loaded with varying amounts of HQS (from 0.073 to 1.22 mmol/g of AG MP-1) show the same bands, similar shapes, and the same peak area ratios ($A_{343\text{ nm}}/A_{388\text{ nm}}$) of 0.89 (Figure 4).

Figure 5 presents normalized absorption spectra of the immobilized HQS (0.5500 mmol/g of AG MP-1) and its Cd complexes at various concentrations. All spectra are composed of two bands. The first band of the immobilized HQS (0.5500 mmol/g of AG MP-1) appearing at 345 nm does not shift, but the other is gradually red-shifted upon increasing Cd concentrations in the resin phase. This phenomenon points to the unique capability of immobilized HQS for complexing Cd, presumably via its negatively charged phenolic oxygen and the nonbonding electrons of the quinoline nitrogen. In the range of 1.18×10^{-4} –0.075 mmol of Cd/g of AG MP-1, the peak ratio is independent of Cd concentration in the resin phase. Thus, the same peak ratio as for uncomplexed AG MP-1-HQS, 0.89 ($A_{345\text{ nm}}/A_{395\text{ nm}}$) is obtained. As Cd concentrations increase, the peak ratio ($A_{345\text{ nm}}/A_{403\text{ nm}}$) decreases, to become 0.80 for 0.157 mmol of Cd/g of AG MP-1 and 0.74 for 0.22 mmol of Cd/g of AG MP-1.

Fluorescence Microscopy Measurements. HQS in the Solid State and Immobilized on AG MP-1. Figure 6 shows the normalized

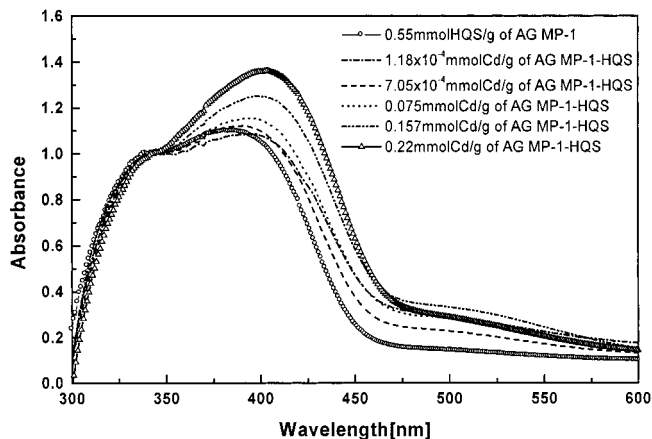


Figure 5. Normalized electronic absorption spectra from AG MP-1-HQS and Cd complexes at various concentrations.

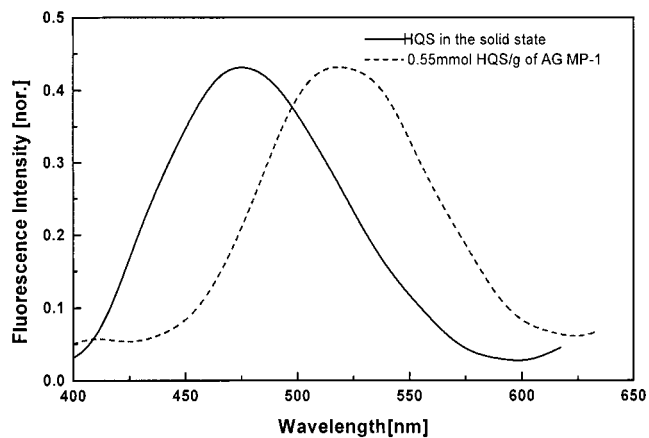


Figure 6. Normalized fluorescence spectra of HQS in the solid state and immobilized HQS on AG MP-1 after two-photon excitation.

two-photon fluorescence spectra of HQS in the solid state and on AG MP-1 (0.5500 mmol/g of AG MP-1), respectively. The maximum emission of HQS in the solid state is located at 475 nm, while the immobilized HQS emits a red-shifted fluorescence with the maximum intensity at 518 nm. To interpret the observed phenomena, we must take into account the structural forms associated with them. When sodium 8-hydroxyquinoline-5-sulfate dihydrate is in the solid state, it presents the same emission as HQS in sulfuric acid.²⁸ Also it should be noted that the fluorescence spectra of HQS in sulfuric acid depend on the concentrations of sulfuric acid in the range of 97–84.7%.²⁹ This result, in agreement with that reported in the literature,²⁸ illustrates that HQS in the solid state is mostly associated by hydrogen bonding and that the proton in the hydrogen bond stems mainly from the SO_3H group and not from the phenolic OH group.

Following immobilization on AG MP-1, HQS exists in the form of deprotonated quinolate (C, Chart 1). As already noted, the immobilization of HQS was done under basic conditions, and the interaction of HQS with the ionic resin is purely electrostatic. The shift to higher wavelength is due to the HQS existing in the quinolate form on the resin.

Imaging the Microdistribution of the Extractant (HQS) and its Cd Complex in the Resin Phases. The use of confocal fluorescence

(28) Viossat, B.; Khodadad, P.; Rodier, N. *Bull. Soc. Chim. Fr.* **1982**, (7–8, Pt. 1), 289–292.

(29) Onoue, Y.; Hiraki, K.; Morishige, K.; Nishikawa, Y. *Nippon Kagaku Kaishi* **1978**, 9, 1237–1243.

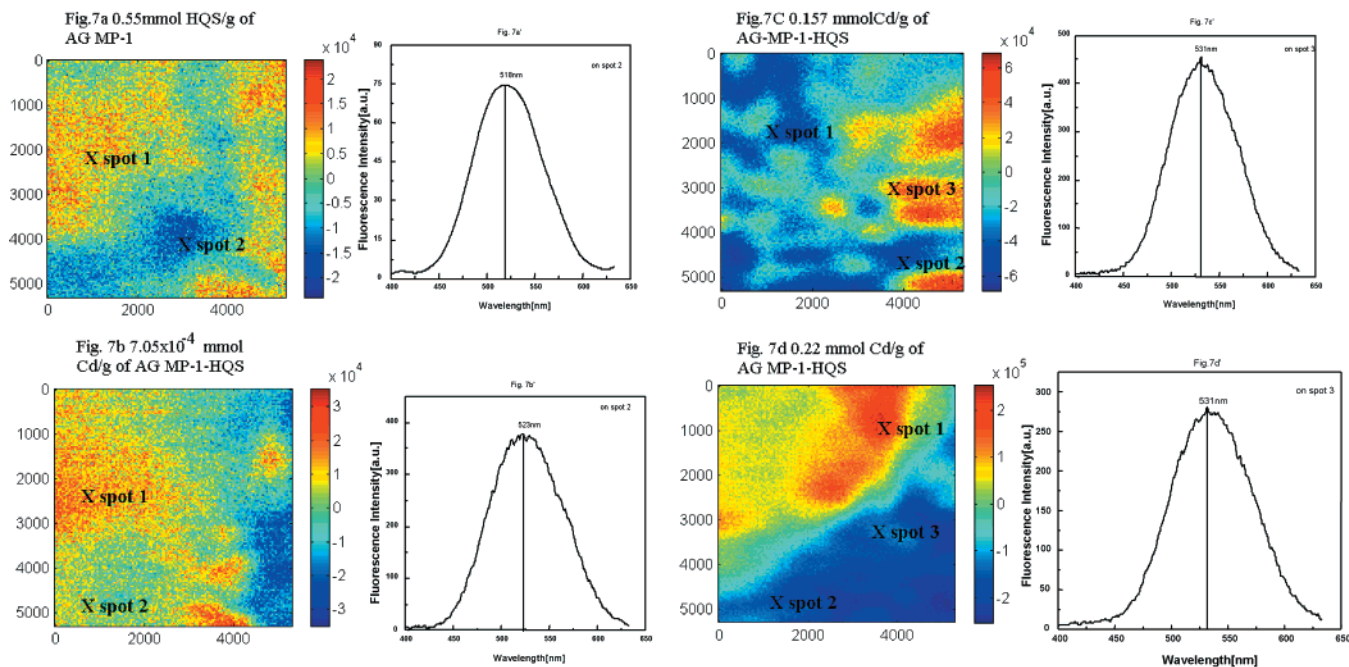


Figure 7. Imaging of the microdistribution of the extractant (HQS) and its Cd complex in the resin phases.

microscopy allows accurate measurement of fluorescence emission from a chosen locus. This technique is a very strong tool to follow the microdistribution of the extractant HQS and its Cd complex in the resin phase. Fluorescence images of $5 \mu\text{m} \times 5 \mu\text{m}$ fields were obtained by scanning the sample and collecting light with an avalanche photodiode. Figure 7a shows an image of extractant HQS (0.5500 mmol/g of AG MP-1) on AG MP-1. Clearly, according to variations of fluorescence intensity within the scanned field, HQS is unevenly distributed. In the same way, images have also been obtained from Cd-complexed AG MP-1, ranging from 7.05×10^{-4} to 0.22 mmol of Cd per gram of AG MP-1-HQS (Figure 7b–d). According to the images in Figure 7, it can be concluded that the fluorescent chelator and metal complexes do not distribute uniformly in the heterogeneous resin. The microdistribution of HQS is dominated by the local $^+\text{NR}_4$ group concentration. Furthermore, Cd complexation *does not* lead to homogenization of the microdistribution of HQS in the resin, e.g., by causing migration of the complex from micropores to macropores. (The initial idea of the study was to use the sensitive fluorescence microspectroscopic method to observe migration of extractant followed by metal ion coordination. Thus, we immobilized metal extractant on ion-exchange resin with the hope that metal salt sorption can break the bond between the extractant and the basic group of the polymer. The fluorescence microspectroscopic method present here does not provide any information about the morphology of the resin. Other methods, such as surface measurements are reported (see ref 30). We intend to combine such a method with confocal microscopy measurements for relating the present results to previous morphological studies.) As a result, the Cd complex is randomly distributed in macropores, micropores or on the surface of the resin phase.

To see whether we can distinguish between fluorescence emission from immobilized free HQS and from its Cd complex,

we measured emission spectra from uncomplexed and complexed AG MP-1-HQS. Figure 7a' shows the spectrum of the immobilized HQS from spot 2, characterized by a maximum emission at 518 nm. This maximum emission at 518 nm, independent of sample uniformity, can be selected as the marker for the immobilized free HQS. Similar spectra [Figure 7b'–d'] were also recorded from samples containing unsaturated and saturated levels of Cd. It is interesting to note that the fluorescence from saturated Cd samples (0.157 and 0.22 mmol of Cd, Figure 7c' and d') shows a relatively red-shifted emission ($\Delta\lambda_{\text{max}} = 531 \text{ nm} - 518 \text{ nm} = 13 \text{ nm}$), proving that the emission is singularly from the Cd complexes. This is a novel and important observation, since it allows direct and proportional correlation between fluorescence intensity and Cd metal concentration, at a wavelength of 531 nm. Consequently, the microenvironment of uncomplexed and complexed AG MP-1-HQS can be distinguished by the fluorescence microspectroscopic method; such characterization cannot be achieved by bulk measurements.

The results shown in Figure 7, display clearly the potential of the fluorescence microspectroscopic method for imaging HQS loaded resins and analyzing the locations of both the fluorescent ligand (HQS) and its Cd complex throughout the resin zones and sublocations. If needed for accurate and full morphological characterization, more zones and spots may be chosen, but the results presented here are sufficient to show the potential of this method to determine the microdistribution of HQS and its Cd complex in the resin phase.

Fluorescence Spectra of Cd-Complexed AG MP-1-HQS and Their Behavior. Spectra from samples containing varying amounts of Cd-complexed AG MP-1-HQS, ranging from 0 to 0.22 mmol of Cd/g of AG MP-1-HQS are presented in Figure 8. Upon increase of Cd concentration in the bulk resin phase, the spectra are gradually red-shifted, and the total fluorescence intensity increases. However, the spectral shifts are dependent on the

(30) Strikovskiy, A. G.; Warshawsky, A.; Hanková, L.; Jerábek, K. *Acta Polym.* **1998**, *49*, 600–605.

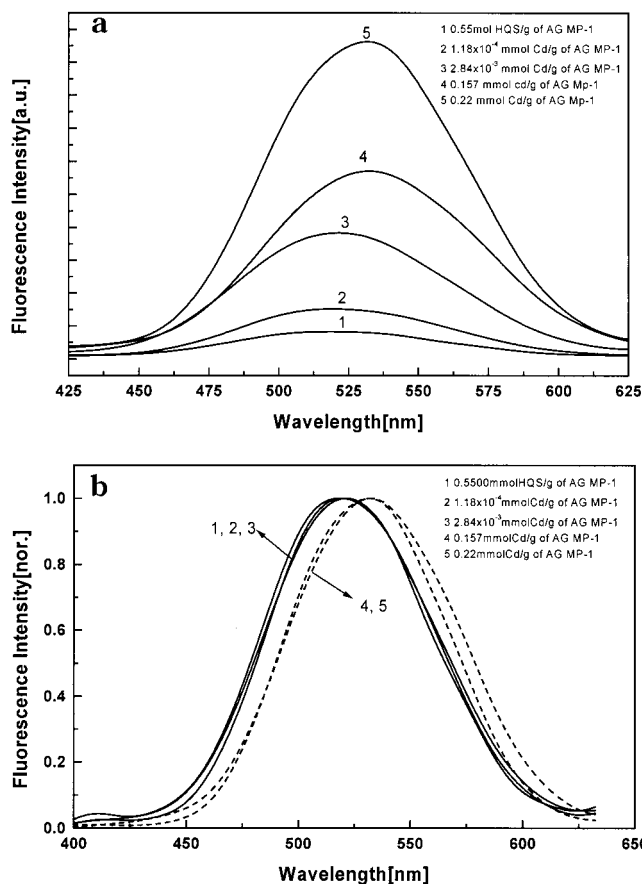


Figure 8. Fluorescence spectra from different concentrations of Cd complexes on AG MP-1-HQS.

amounts of Cd in the resin phase. When the limit of Cd concentration is lower than 2.84×10^{-3} mmol/g of AG MP-1, the maximum emission is around 520 nm, and when the Cd concentration is higher than 0.157 mmol/g of AG MP-1, the spectra is red-shifted to the same wavelength. This increase in fluorescence intensity is not a linear relationship with bulk Cd concentrations, but it can form the basis for qualitative analysis of Cd in the resin phase. The fluorescence microspectroscopic method may thus be further developed for quantitative analysis of Cd on the microscale.

Photobleaching of HQS and Cd Complex in the Resin Phase. To carry out quantitative Cd measurements, it is of importance to examine the photostability of HQS and the Cd complex on the resin phase. Following the fluorescence images taken in a $5 \mu\text{m} \times 5 \mu\text{m}$ field, fluorescence intensity was continuously recorded on various spots (labeled in Figure 7). As an example, Figure 9 displays the unnormalized and normalized time-dependent fluorescence intensities from three spots on a 0.157 mmol of Cd/g of AG MP-1-HQS sample (see Figure 7c). The time evolution of data from the sample is reasonably well-fitted to an exponential function, to give an effective photobleaching rate. The same photobleaching experiments were carried out on samples with average Cd concentrations ranging from 0 to 0.22 mmol/g of AG MP-1-HQS. The photobleaching occurs not only in Cd-complexed samples but also in the uncomplexed AG MP-1-HQS. It appears that the time-dependent decrease of the fluorescence is correlated with the fluorescence intensity distribution: the fluorescence from brighter spots decays more slowly than the fluorescence from darker spots. The fluorescence decay curves measured on

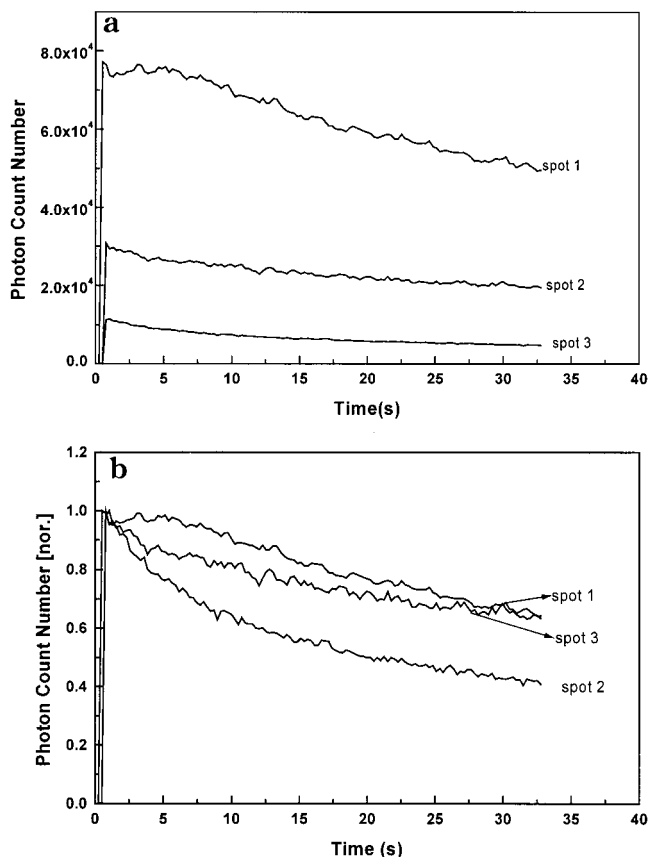


Figure 9. Unnormalized and normalized fluorescence intensity from various spots on the sample, plotted as a function of time.

intermediate-intensity spots show a double-exponential decrease of fluorescence intensity. This indicates that at least two different processes contribute to the photobleaching reaction, and their relative contribution depends on the microenvironment, possibly due to inhomogeneous distribution of Cd ions.

CONCLUSIONS

The goal of this work was to study chromophoric "chelate-forming" resins by an optical spectral method for the assessment of microenvironment factors on metal binding, resin characterization, and possibly sensing Cd. Fluorescence microspectroscopy provides a convenient platform to image the microdistribution of chelator and its Cd-complexed groups in the resin phase and to distinguish between the fluorescence chelator and its Cd complex on microscale. It was found that the immobilized HQS and Cd complex are nonuniformly distributed in the resin phases. The photobleaching phenomenon that was observed involves not only the immobilized HQS but also Cd complexes. Variation of photobleaching rates among samples and in the same sample further confirms the microdistribution of HQS and its Cd complex in different microenvironments, with yet undefined chemical reactions occurring following photoexcitation. To correlate the effective photobleaching rate to bulk Cd concentration and to expand the study toward HQS complexes of other metal ions remains an object for further studies.

Received for review December 12, 2000. Accepted May 16, 2001.

AC001465A